Supporting Information

Graphene-Based Mesoporous SnO_2 Nanosheets as Multi-Functional Hosts for High Performance Lithium-Sulfur Batteries

Shengtang Liu, [‡,†,§] *Ce Zhang,* [‡,§] *Wenbo Yue,*[*,†] *Xi Chen*[†]*, and Xiaojing Yang*[*,†]

[†]Beijing Key Laboratory of Energy Conversion and Storage Materials, College of Chemistry Beijing Normal University, Beijing, 100875, P. R. China

[§]Qian Xuesen Laboratory of Space Technology, China Academy of Space Technology (CAST), Beijing, 100094, P. R. China

* Corresponding author

E-mail: wbyue@bnu.edu.cn (W. B. Yue), yang.xiaojing@bnu.edu.cn (X. J. Yang)

Experimental Section

Preparation of graphene oxide (GO) and graphene (GN)

5 g of graphite powder and 5 g of $NaNO_3$ were added into 230 mL of 98% H_2SO_4. After stirring in an ice bath for 15 min, 30 g of $KMnO_4$ was slowly added to the mixture under stirring for 15 min below 5 °C. The mixture was then heated at 35 °C for 30 min. Subsequently, 460 mL of distilled water was slowly added into the above mixture, and the mixture was stirred at 98 °C for more than 15 min. The mixture was then diluted with 1400 mL of distilled water and the reaction was terminated by adding 25 mL of 30 % H_2O_2. Meanwhile, the colour of the solution turned from dark brown to bright yellow. The resulting mixture was filtered and washed with distilled water three times to remove residual acids and salts. The as-synthesized GO was dispersed in water by ultrasonication for 30 min, and the aggregated GO nanosheets were removed by a low-speed centrifugation. GN was synthesized by reduction of GO under thermal treatment with N_2 protection at 600 °C for 2 h.

Sample characterization

The morphologies of the samples were studied by a field emission scanning electron microscopy (FESEM, S-8010, Hitachi) equipped with an energy-dispersive X-ray microanalysis (EDX) system and a FEI Talos 200S transmission electron microscopy (TEM) operated at 200 kV. X-ray diffraction (XRD) patterns were characterized by a PANalytical X' Pert PRO MPD X-ray diffractometer using a Cu Kα radiation source. The thermogravimetric analysis was performed on a NETZSCH STA 409 PC/PG thermal analyzer under N_2 atmosphere. Nitrogen sorption isotherms were recorded on a Quadrasorb SI (Quantachrome, USA) sorption analyzer at 77 K. The specific surface area was calculated using the Brunauer-Emmett-Teller (BET) method and the pore size distribution was determined using the non-local density functional theory (NLDFT) method.

Electrochemical measurements

The Li-S half-cell test was assembled using CR-2032 coin cells, which were fabricated in an argon-filled glovebox (UniLab, Mbraun, [O_2] <0.1 ppm, [H_2O] <0.1 ppm). Li foil was used as both the counter and reference electrode, and microporous membrane (Celgard 2400) as the

separator, respectively. 1 M lithium bis(tri-fluoromrthanesulfonyl)imide (LiTFSI) in a mixed solution of 1,3-dioxolane (DOL) and 1,2-dimethoxyethane (DME) (volume ratio 1:1) containing 2 wt % $LiNO_3$ was used as the electrolyte. The amount of electrolyte added in the cell is ~40 μL. The galvanostatic charge and discharge tests of the cells were performed by a LAND CT2001A battery-testing instrument in the voltage range of 1.7 to 2.8 V (versus Li/Li^+) at room temperature. Cyclic voltammetry (CV) was carried out on a Bio-Logic VMP3 electrochemical analyzer at a scan rate of 0.2 mV s^{-1}. The electrochemical impedance spectroscopy (EIS) study was performed by the same electrochemical analyzer with the frequency range from 100 kHz to 10 mHz at an AC amplitude of 5 mV.

The electrodes for symmetrical cells were prepared without sulfur loading. Host material (GN, $mSnO_2$ and G-$mSnO_2$) and PVDF binder at weight rate of 4:1 were dispersed in NMP. The mixture was dropped on carbon papers (a diameter of 14mm) and dried at 100 ºC for 12 hours. The host material-coated carbon papers were used as working and counter electrodes, while 40 uL electrolyte containing 0.5 mol L^{-1} Li_2S_6 was added. The electrolyte was prepared by adding Li_2S and S at molar ratio of 1:5 into the corresponding solvent (see the electrolyte for Li-S half-cell test). CV measurements of the symmetrical cells were performed at a scan rate of 50 mV s^{-1} from -0.9 to 0.9 V. The electrochemical impedance spectroscopy (EIS) study was performed by the same electrochemical analyzer with the frequency range from 100 kHz to 10 mHz at an AC amplitude of 5 mV.

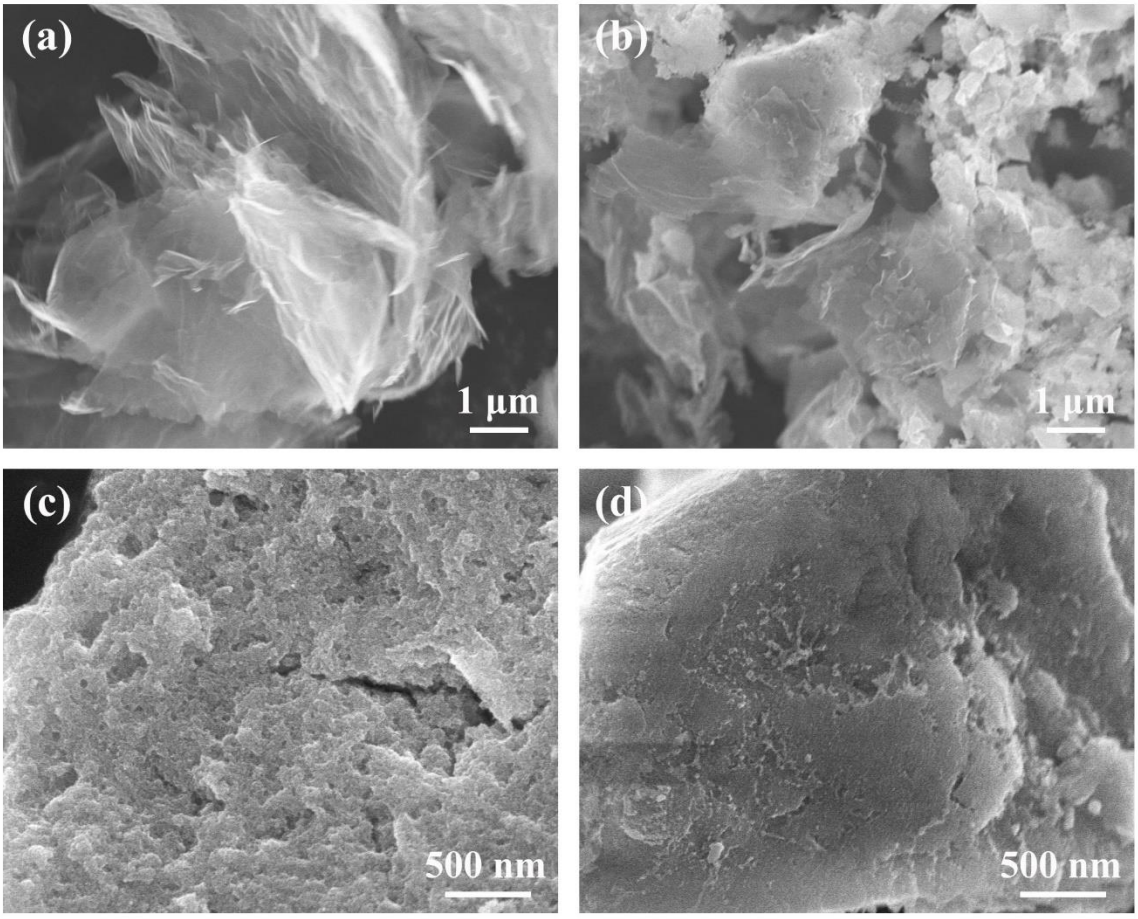

Figure S1. SEM images of (a) GN, (b) GN@S, (c) $mSnO_2$ and (d) $mSnO_2$@S.

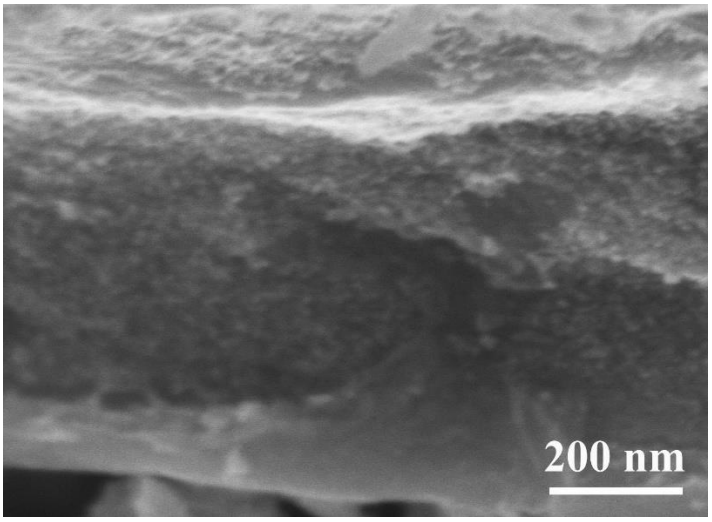

Figure S2. Cross-section SEM image of G-$mSnO_2$. The cross-sectional view is a little difficult because of the flexible graphene substrate.

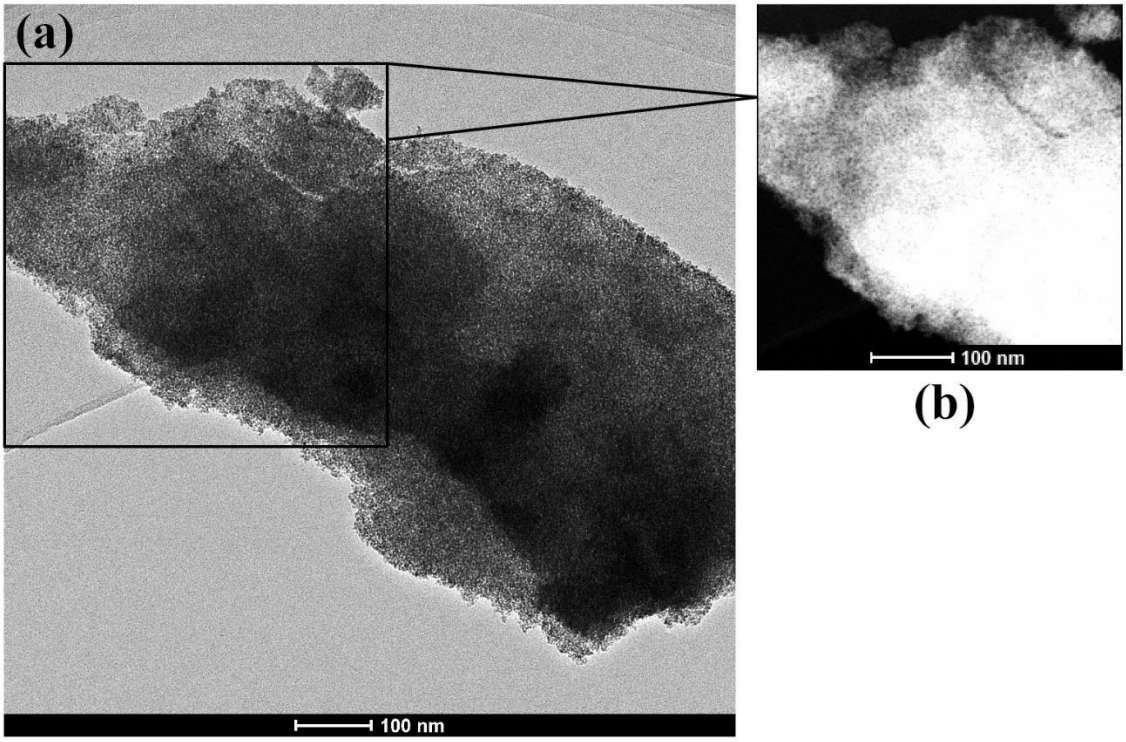

Figure S3. (a) STEM and (b) HAADF images of G-mSnO_2@S.

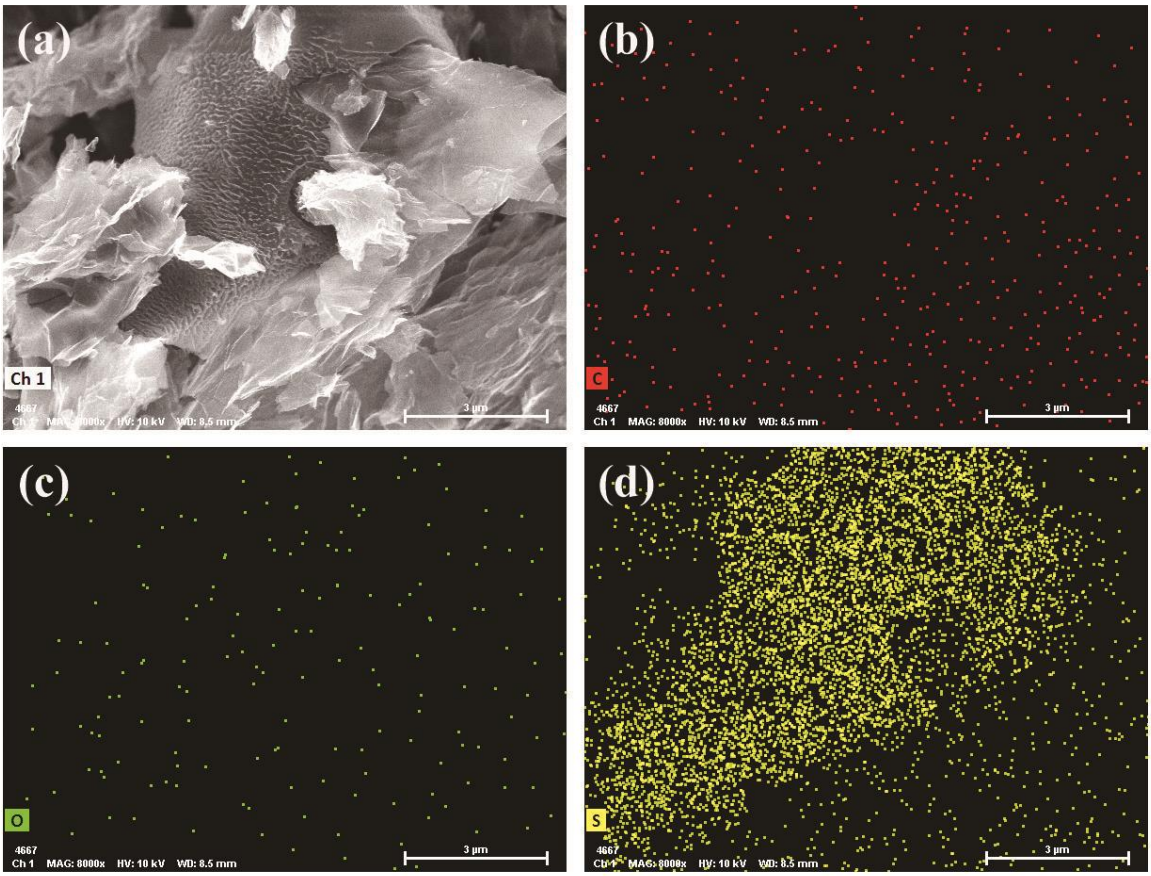

Figure S4. (a) SEM image of GN@S and (b-d) corresponding EDX mapping images of C, O and S elements.

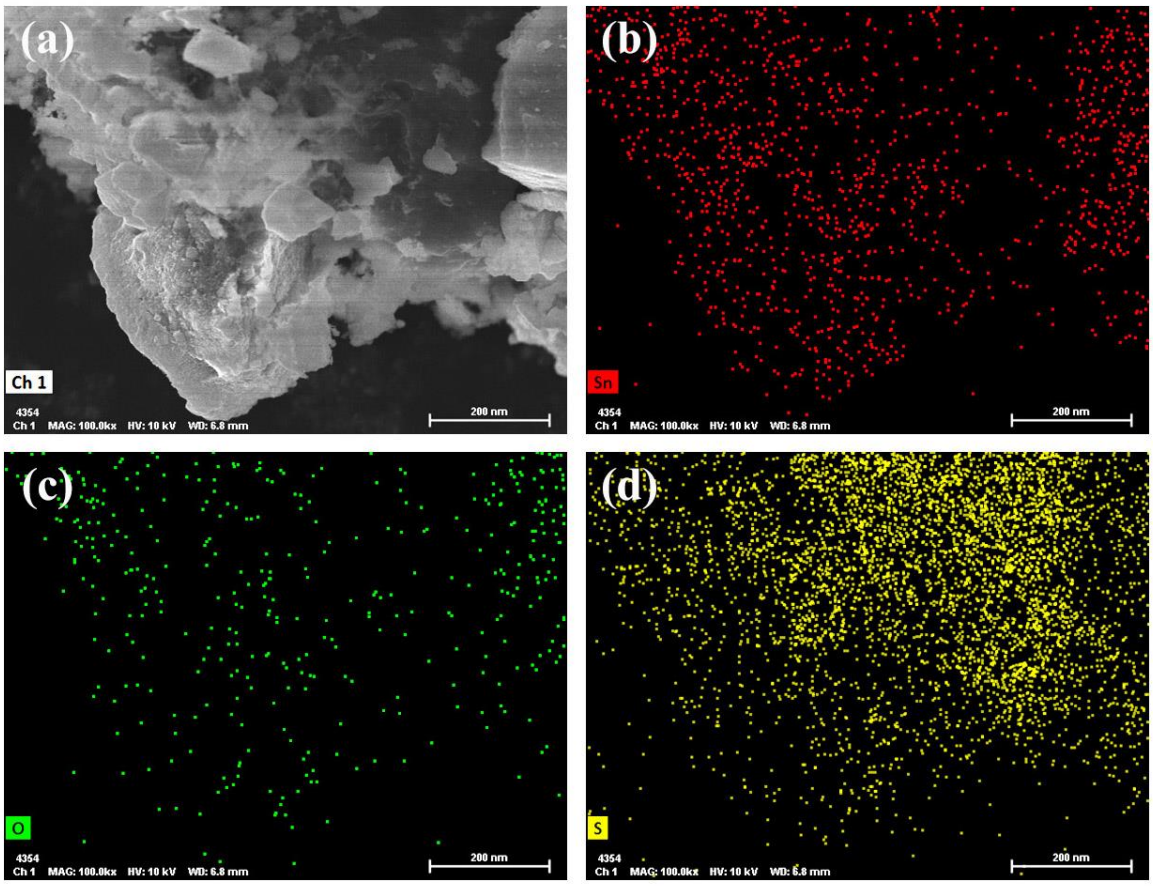

Figure S5. (a) SEM image of mSnO_2@S and (b-d) corresponding EDX mapping images of Sn, O and S elements.

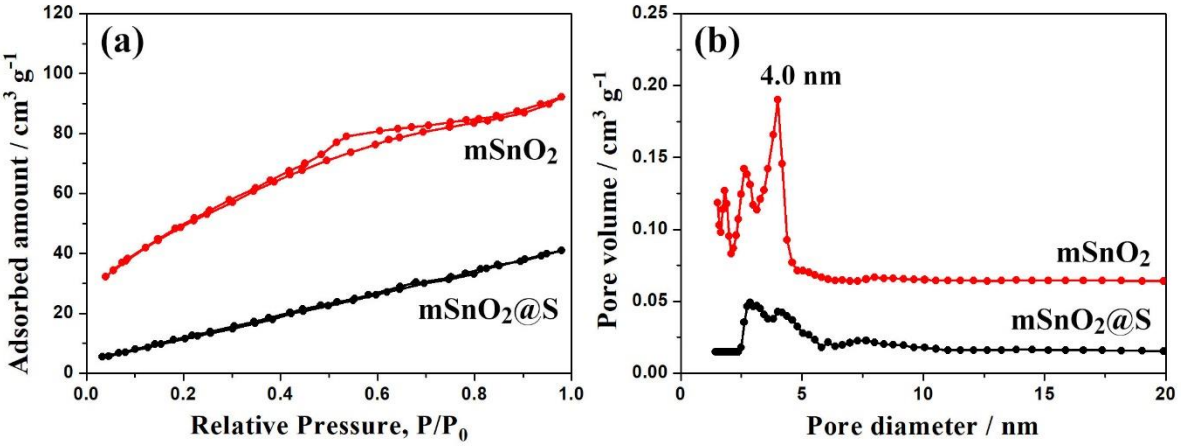

Figure S6. (a) N_2 adsorption/desorption isotherms and (b) pore size distributions of $mSnO_2$, and $mSnO_2$@S.

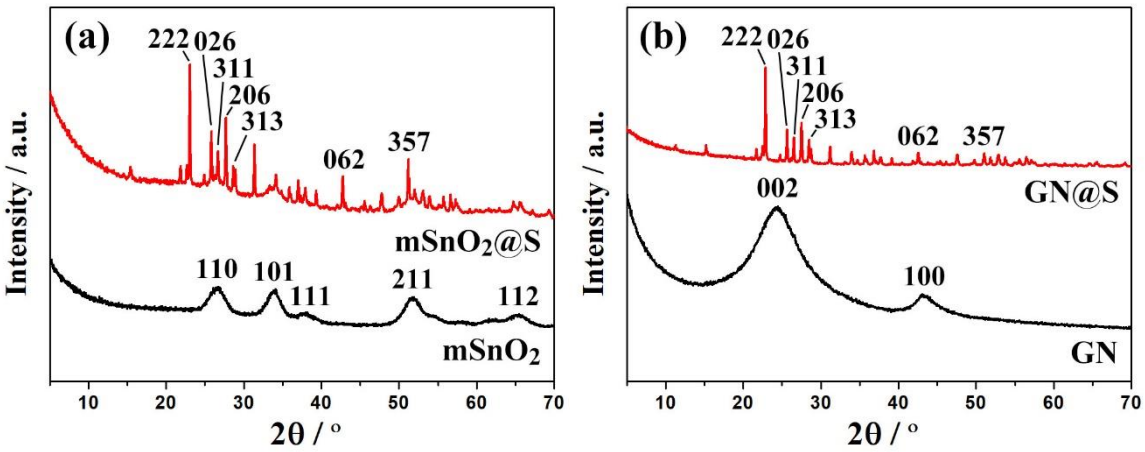

Figure S7. XRD patterns of (a) $mSnO_2$, $mSnO_2$@S and (b) GN, GN@S.

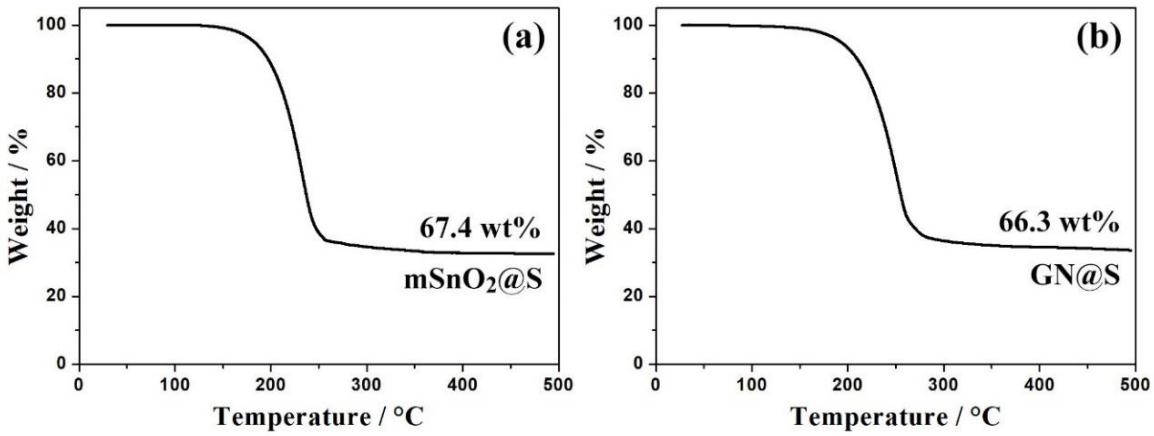

Figure S8. TGA curves of (a) $mSnO_2$@S and (b) GN@S.

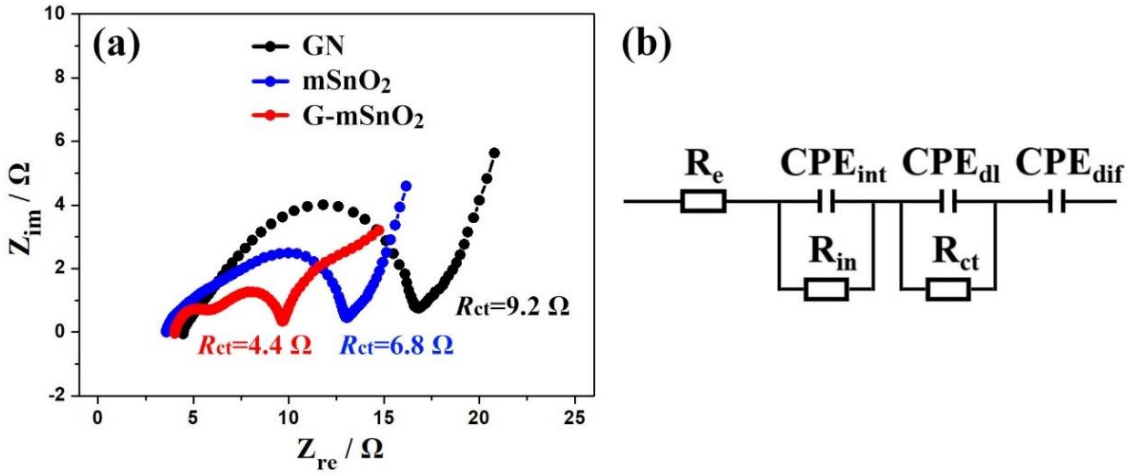

Figure S9. (a) EIS spectra of the symmetrical battery with identical electrode. (b) The equivalent circuit for $mSnO_2$@S, GN@S and G-$mSnO_2$@S electrodes.

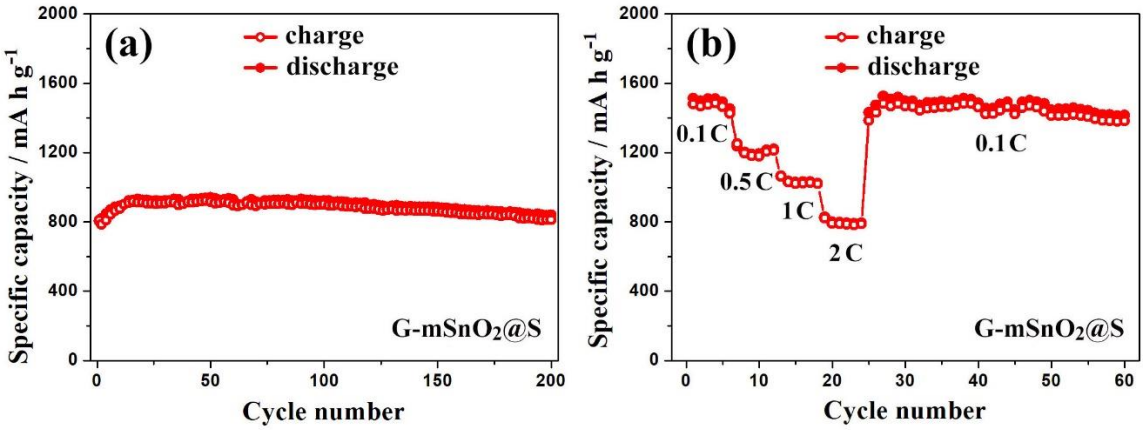

Figure S10. (a) The cycle performance of G-mSnO_2@S with higher sulfur content (78 wt%) and mass loading (4.2 mg cm^{-2}) at 0.1 C. (b) Rate performance of G-mSnO_2@S at 0.1-2 C.

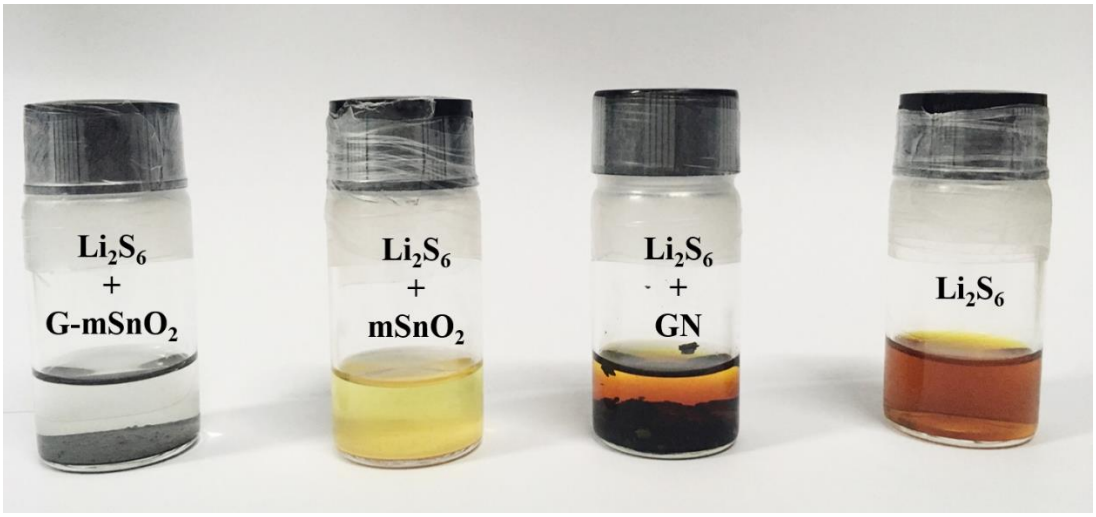

Figure S11. Digital photographs of the Li_2S_6 adsorption measurement with G-mSnO_2, mSnO_2 and GN.

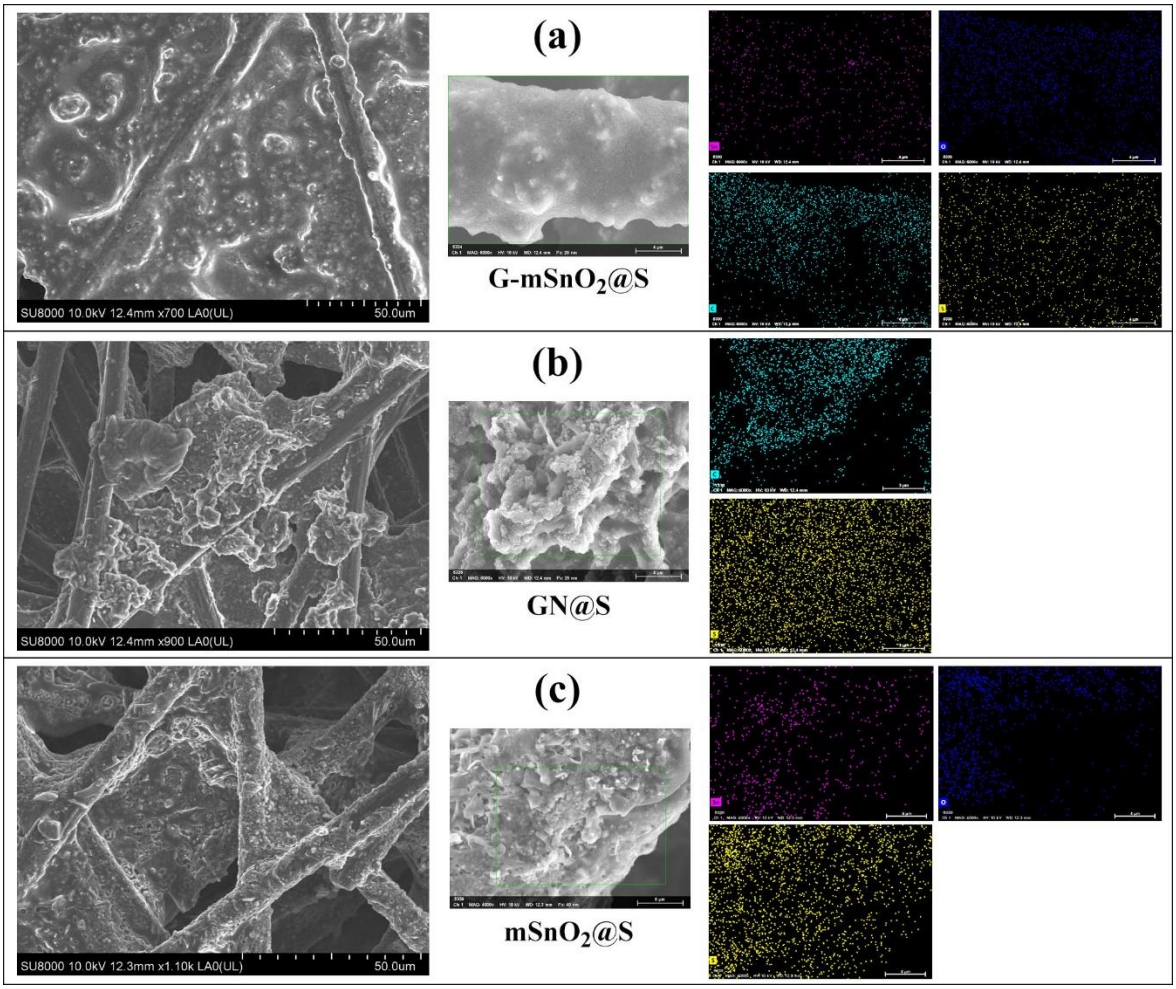

Figure S12. SEM-EDX mapping images of (a) G-mSnO_2@S, (b) GN@S and (c) mSnO_2@S. The images on the left and in the middle are SEM images at low and high magnifications, respectively.

Table S1. Surface areas, pore volumes and pore sizes of G-mSnO_2, G-mSnO_2@S, mSnO_2, mSnO_2@S, GN and GN@S.

Sample	Surface area / $m^2\ g^{-1}$	Pore volume / $cm^3\ g^{-1}$	Pore size / nm
G-mSnO_2	214.0	0.23	3.9
G-mSnO_2@S	29.1	0.03	N/A
m-SnO_2	173.2	0.16	4.0
m-SnO_2@S	64.1	0.07	N/A
GN	104.7	0.12	N/A
GN@S	12.6	0.01	N/A

Table S2. The electrolyte resistance (R_e), interphase contact resistance (R_{int}) and charge-transfer resistances (R_{ct}) of GN@S, mSnO_2@S and G-mSnO_2@S.

Sample	R_e / Ω	R_{int} / Ω	R_{ct} / Ω
GN@S	7.6	20.0	3.6
mSnO_2@S	10.4	127.1	242.1
G-mSnO_2@S	5.3	43.0	10.6

Table S3. Electrochemical performance comparison of G-mSnO_2@S with reported electrode materials for Li-S batteries.

Electrode material	Voltage window	Sulfur loading	Electrochemical performance	Ref
V_2O_5/graphene	1.8V-3.2V	75%	600 mA h g^{-1} (0.5C, 280 cycles)	1
TiO_2/graphene	1.7V-2.8V	72%	1116 mA h g^{-1} (0.2C, 100 cycles)	2
ITO-carbon	1.7V-2.6V	57%	1034 mA h g^{-1} (0.2C, 200 cycles)	3
SnO_2@C	1.7V-2.8V	58%	763 mA h g^{-1} (0.2 A g^{-1}, 100 cycles)	4
MnO_2	1.7V-3.0V	75%	900 mA h g^{-1} (0.2C, 200 cycles)	5
CoOH/LDH	1.7V-2.8V	75%	653 mA h g^{-1} (0.1C, 100 cycles)	6
SnS/C	1.8V-2.8V	78%	750 mA h g^{-1} (0.5C, 300 cycles)	7
SnO_2/C	1.8V-2.8V	74%	600 mA h g^{-1} (0.5C, 50 cycles)	7
Fe_2O_3/graphene	1.7V-3.0V	60%	400 mA h g^{-1} (2C, 500 cycles)	8
MoS_x/graphene	1.8V-2.6V	75%	628 mA h g^{-1} (0.5C, 600 cycles)	9
SnO/CNT/S	1.7V-2.8V	70%	530 mA h g^{-1} (0.5C, 1000 cycles)	10
C@SnO_2/S	1.7V-2.8V	11%	560 mA h g^{-1} (2C, 1000 cycles)	11
NCNT@Co-SnS_2	1.7V-2.8V	N/A	1004 mA h g^{-1} (0.1C, 100 cycles)	12
$ZnCo_2O_4$@N-rGO	1.7V-2.8V	71%	760 mA h g^{-1} (0.8 A g^{-1}, 200 cycles)	13
G-mSnO_2@S	1.7V-2.8V	69%	1380 mA h g^{-1} (0.1C, 200 cycles) 680 mA h g^{-1} (2C, 500 cycles)	our work

Reference

(1) Liang, X.; Kwok, C. Y.; Lodi-Marzano, F.; Pang, Q.; Cuisinier, M.; Huang, H.; Hart, C. J.; Houtarde, D.; Kaup, K.; Sommer, H.; Brezesinski, T.; Janek, J.; Nazar, L. F., Tuning Transition Metal Oxide-Sulfur Interactions for Long Life Lithium Sulfur Batteries: The "Goldilocks" Principle. *Adv. Energy Mater.* **2016**, 6 (6), 1501636.

(2) Li, Y.; Cai, Q.; Wang, L.; Li, Q.; Peng, X.; Gao, B.; Huo, K.; Chu, P. K., Mesoporous TiO_2 Nanocrystals/Graphene as an Efficient Sulfur Host Material for High-Performance Lithium-Sulfur Batteries. *ACS Appl. Mater. Interface.* **2016**, 8 (36), 23784-23792.

(3) Yao, H.; Zheng, G.; Hsu, P.-C.; Kong, D.; Cha, J. J.; Li, W.; Seh, Z. W.; McDowell, M. T.; Yan, K.; Liang, Z.; Narasimhan, V. K.; Cui, Y., Improving lithium-sulphur batteries through spatial control of sulphur species deposition on a hybrid electrode surface. *Nat. Commun.* **2014**, 5, 3943.

(4) Cao, B.; Li, D.; Hou, B.; Mo, Y.; Yin, L.; Chen, Y., Synthesis of Double-Shell SnO_2@C Hollow Nanospheres as Sulfur/Sulfide Cages for Lithium-Sulfur Batteries. *ACS Appl. Mater. Interface.* **2016**, 8 (41), 27795-27802.

(5) Liang, X.; Hart, C.; Pang, Q.; Garsuch, A.; Weiss, T.; Nazar, L. F., A highly efficient polysulfide mediator for lithium-sulfur batteries. *Nat. Commun.* **2015**, 6, 5682.

(6) Zhang, J.; Hu, H.; Li, Z.; Lou, X. W., Double-Shelled Nanocages with Cobalt Hydroxide Inner Shell and Layered Double Hydroxides Outer Shell as High-Efficiency Polysulfide Mediator for Lithium-Sulfur Batteries. *Angew. Chem. Int. Ed.* **2016**, 55 (12), 3982-3986.

(7) Li, X.; Lu, Y.; Hou, Z.; Zhang, W.; Zhu, Y.; Qian, Y.; Liang, J.; Qian, Y., SnS_2- Compared to SnO_2-Stabilized S/C Composites toward High Performance Lithium Sulfur Batteries. *ACS Appl. Mater. Interface.* **2016,** 8 (30), 19550-19557.

(8) Zheng, C.; Niu, S.; Lv, W.; Zhou, G.; Li, J.; Fan, S.; Deng, Y.; Pan, Z.; Li, B.; Kang, F.; Yang, Q.-H., Propelling polysulfides transformation for high-rate and long-life lithium sulfur batteries. *Nano Energy* **2017**, 33, 306-312.

(9) Lin, H.; Yang, L.; Jiang, X.; Li, G.; Zhang, T.; Yao, Q.; Zheng, G. W.; Lee, J. Y., Electrocatalysis of polysulfide conversion by sulfur-deficient MoS_2 nanoflakes for lithium-sulfur batteries. *Energy Environ. Sci.* **2017**, 10 (6), 1476-1486.

(10) Kim, A. Y.; Kim, M. K.; Kim, J. Y.; Wen, Y.; Gu, L.; Van-Duong, D.; Choi, H.-S.; Byun, D.; Lee, J. K., Ordered SnO nanoparticles in MWCNT as a functional host material for high-rate lithium-sulfur battery cathode. *Nano Research* **2017**, 10 (6), 2083-2095.

(11) Wang, M.; Fan, L.; Wu, X.; Tian, D.; Cheng, J.; Qiu, Y.; Wu, H.; Guan, B.; Zhang, N.; Sun, K.; Wang, Y., Hierarchical mesoporous SnO_2 nanosheets on carbon cloth toward enhancing the polysulfides redox for lithium-sulfur batteries. *J. Mater. Chem. A.* **2017**, 5 (37), 19613-19618.

(12) Cao, X.; Yang X.; Li, M.; Li, J.; Luo, J.; wang, J.; Sun, X., Cobalt-Doped SnS_2 with Dual Active Centers of Synergistic Absorption Catalysis Effect for High-S Loading Li-S Batteries. *Adv. Funct. Mater*. **2019**, 1806724.

(13) Sun, Q.; Xi, B.; Li, J.-Y.; Mao, H.; Ma, X.; Liang, J.; Feng, J.; Xiong, S., Nitrogen-Doped Graphene-Supported Mixed Transition-Metal Oxide Porous Particles to Confine Polysulfides for Lithium-Sulfur Batteries. *Adv. Energy Mater*. **2018,** 8 (22), 1800595.